The Cationic Porphyrin TMPyP4 Down-Regulates c-*MYC* and Human Telomerase Reverse Transcriptase Expression and Inhibits Tumor Growth *in Vivo*[1]

Cory L. Grand, Haiyong Han, Rubén M. Muñoz, Steve Weitman, Daniel D. Von Hoff, Laurence H. Hurley, and David J. Bearss[2]

Arizona Cancer Center, Tucson, Arizona 85724 [C. L. G., H. H., R. M. M., D. D. V. H., L. H. H., D. J. B.]; Institute for Drug Development, San Antonio, Texas 78245 [S. W.]; and College of Pharmacy, The University of Arizona, Tucson, Arizona 85721 [C. L. G., L. H. H.]

Abstract

Cationic porphyrins are being studied as possible anticancer agents because of their ability to bind to and stabilize DNA guanine quadruplexes (G-quadruplexes). We have shown previously that the cationic porphyrin TMPyP4 is able to bind to and stabilize G-quadruplexes in human telomere sequences, resulting in inhibition of telomerase activity. To better understand the mechanism of action behind telomerase inhibition by TMPyP4, we performed a cDNA microarray analysis on cells treated with TMPyP4 and TMPyP2, a positional isomer of TMPyP4 that has low affinity for G-quadruplexes. Analysis of time course data from the microarray experiments revealed that TMPyP4 and TMPyP2 treatment altered the expression of several gene clusters. We found that c-*MYC*, an oncogene nearly ubiquitous in human tumors that bears the potential in its promoter to form a G-quadruplex, was among the genes specifically down-regulated by TMPyP4, but not by TMPyP2. The *hTERT* gene, which encodes the catalytic subunit of telomerase, is transcriptionally regulated by c-MYC, and we have found that TMPyP4 also causes a decrease in human telomerase reverse transcriptase transcripts, suggesting two possible mechanisms for the effect of TMPyP4 on telomerase activity. We also show that TMPyP4, but not TMPyP2, is able to prolong survival and decrease tumor growth rates in two xenograft tumor models. We believe that, because of the actions of TMPyP4 in decreasing both c-MYC protein levels and telomerase activity, as well as its anticancer effects *in vivo*, it is a worthwhile agent to pursue and develop further.

Introduction

G-quadruplexes have been implicated in a number of processes, including inhibition of telomerase and control of gene expression (1–7). We have demonstrated previously that the G-quadruplex-interactive compound TMPyP4 (Fig. 1) can inhibit telomerase in a cell-free system and *in vitro* in cell lines incubated with TMPyP4 (8). More recently, we have demonstrated that multiple myeloma cell lines exhibit telomere shortening, delayed cell crisis, and apoptosis consistent with telomeres reaching a critical length.[3] In sea urchin cells, we have demonstrated the formation of anaphase bridges after incubation with TMPyP4, which we interpret as resulting from dimerization of single-stranded guanine hairpins (9). All of these results can be rationalized based upon the assumption of direct interaction of TMPyP4 with G-quadruplex structures formed in telomeres. We have demonstrated recently that TMPyP4 can also interact with and stabilize i-motif structures (10), which are interdigitated cytosine-cytosine dimers that form four-stranded structures in the C-rich strand of telomeres and other G-quadruplex-forming sequences (11, 12). Although these i-motifs might not be expected to directly inhibit telomerase, their formation could make the G-rich single strand available to form quadruplexes in telomeres or in duplex regions of guanine-rich/cytosine-rich strands such as those found in the promoters of certain oncogenes. c-*MYC* is one such oncogene that bears a G-quadruplex-amenable sequence in its promoter.

The protein product of the c-*MYC* proto-oncogene transcriptionally activates hTERT,[4] the catalytic subunit of telomerase (13–15), and controls a variety of genes that together enhance the proliferative capacity of cells (16–18). Thus, it is not surprising that c-*MYC* is tightly controlled by a complex mechanism involving four promoters (19, 20). Dysregulation of the c-*MYC* proto-oncogene can arise from a variety of mechanisms, including chromosomal translocation (21), retroviral transduction (22–24), gene amplification (25), and proviral insertion (26). c-*MYC* is overexpressed in a variety of human malignancies, including leukemias, lymphomas, and prostate, lung, breast, pancreatic, ovarian, cervical, and gastric cancers (27–29). Because of its prevalence in human cancers, c-*MYC* is a viable target for anticancer therapeutics.

As a first step to c-*MYC* activation, disruption of the chromatin structure is required to allow access of the transcriptional machinery to the promoter (30). Several nuclease hypersensitivity elements have been shown to play important roles in this process. Notably, one of these, NHE III_1, accounts for 95% of total c-*MYC* transcription (31). This element is unusual in that it is guanine-rich on one strand and

Received 2/8/02; revised 4/8/02; accepted 5/2/02.
[1] This research was supported by grants from the NIH and the Arizona Disease Control Research Commission.
[2] To whom requests for reprints should be addressed, at Arizona Cancer Center, 1515 North Campbell Avenue, Tucson, AZ 85724. Phone: (520) 626-8452; Fax: (520) 626-6898; E-mail: dbearss@azcc.arizona.edu.

[3] M. A. Shammas, R. B. Batchu, J. Y. Wang, L. H. Hurley, R. J. S. Reis, and N. C. Munshi. Telomerase inhibition and cell growth arrest following porphyrin treatment of multiple myeloma cells, submitted for publication.
[4] The abbreviations used are: hTERT, human telomerase reverse transcriptase; NHE, nuclease hypersensitivity element; TRAP, telomerase repeat amplification protocol; RT-PCR, reverse transcription-PCR; q.d., every day; GAPDH, glyceraldehyde-3-phosphate dehydrogenase.

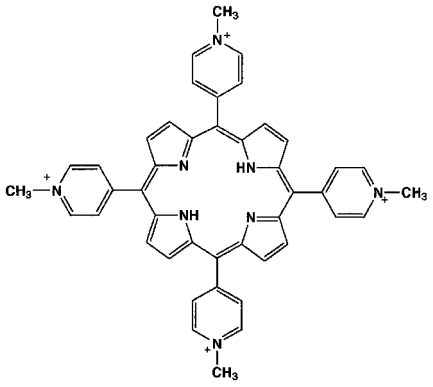

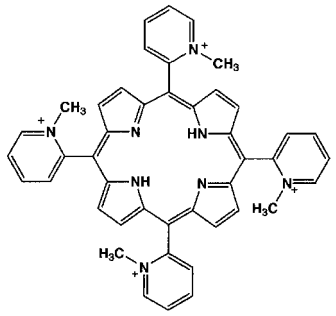

Fig. 1. Structures of the two cationic porphyrins used in this study, 5,10,15,20-tetra-(*N*-methyl-4-pyridyl)porphine (*TMPyP4*) and 5,10,15,20-tetra-(*N*-methyl-2-pyridyl)porphine (*TMPyP2*).

cytosine-rich on the other strand. Both strands are known to form unusual DNA structures; the G-rich strand forms a G-quadruplex (6, 7), and the C-rich strand forms an i-motif or i-tetraplex structure (32). *In vitro*, the G-quadruplex structure that is favored at physiological conditions is a unimolecular, antiparallel, foldover structure (6).

In the present study, we demonstrate that TMPyP4 down-regulates c-*MYC*, and this appears to contribute to the observed effects on telomerase by lowering *hTERT* expression. Consistent with its relative ability to bind to G-quadruplexes, TMPyP2 (Fig. 1), a positional isomer of TMPyP4 that shows much weaker biological activity than TMPyP4, is also less able to down-regulate c-*MYC* and *hTERT*. This effect does not appear to be mediated through a general blockage of the cell cycle, because TMPyP4 does not change the cycling profile of treated cells. We also show that TMPyP4 can relieve tumor burden in both a mammary and neuroblastoma mouse model and increase the life span of tumor-bearing mice, making it a promising lead compound that merits further study.

Materials and Methods

Cell Culture. HeLa S_3 (human cervical carcinoma metastasis) and MiaPaCa-2 (human pancreatic tumor) were obtained from American Type Culture Collection; ForF cells (human foreskin fibroblast cells) were prepared fresh at the Arizona Cancer Center from newborn foreskins. ForF cells and MiaPaCa-2 cells were cultured at 37°C in RPMI 1640 (Cellgro) with 10% fetal bovine serum, 50 units/ml penicillin G sodium, and 50 units/ml streptomycin sulfate (Life Technologies, Inc.). HeLa S_3 cells were cultured in DMEM (Cellgro) with 10% fetal bovine serum, 50 units/ml penicillin G sodium, and 50 units/ml streptomycin sulfate. Cells were grown to 80% confluency and passaged at 1:10 in the following fashion. The medium was aspirated by vacuum, and the cells were washed with 1× PBS (Cellgro). Sufficient trypsin (Life Technologies, Inc.) was added to cover the cells, and cells were incubated at room temperature for ~3 min or until cells detached from the flask with firm tapping. The trypsin was neutralized with an equal volume of culture medium, and the cells were counted using a hemocytometer. Cells (2×10^5 to 1×10^6) were removed for cell cycle analysis. The remaining cells were then pelleted from this mixture by centrifugation at 500 × *g,* the supernatant was aspirated, and the pellet was washed in PBS, recentrifuged, and frozen at −80°C.

Treatment with Drugs. Cell cultures were permitted to reach ~50% confluency before drug was added. Drug concentrations were as follows: 100 μM TMPyP2 and TMPyP4 (synthesized in the laboratory; this dose was shown to be biologically effective in preliminary studies); 0.2 mg/ml doxorubicin (Ben Venue Laboratories, Inc.); 100 nM Taxotere/docetaxel (Rhône-Poulenc Rorer Pharmaceuticals, Inc.); and 10 nM gemcitabine/Gemzar (Eli Lilly and Co.). Drugs were diluted in medium in which the cells were normally cultured. Cells were washed once with PBS, and new medium containing drug was added directly to the flask. Cells were harvested as noted above, 12, 24, 36, 48, or 50 h after initial treatment, concurrently with untreated cells. Time points were collected in duplicate for each treatment.

RNA Extraction. Cell pellets were lysed in Buffer RLT from the RNeasy RNA Mini Extraction kit (QIAGen) and homogenized using a QIAShredder (QIAGen). RNA was extracted according to the protocol included with the RNA Extraction kit and eluted in distilled, deionized water with 0.1% diethyl pyrocarbonate (DEPC-H_2O; Sigma) to a final volume of 30 μl. RNA was quantitated by UV spectrophotometry and stored at −80°C.

Protein Extraction and Quantitation. Cell pellets were lysed in 100–150 μl of NP40 lysis buffer [50 mM Tris-HCl (pH 8.0), 150 mM NaCl, 0.02% sodium azide, 100 μg/ml phenylmethylsulfonyl fluoride, and 1% NP40], the lysates were centrifuged at >14,000 × *g*, and the supernatants were collected and stored frozen at −80°C. Lysates were quantified in 96-well plates by BCA Protein Assay (Pierce).

TRAP Assays. 1.5 μl of protein was used to determine the amount of active telomerase enzyme in each total protein extract, using the TRAPeze radioisotopic detection kit (Intergen), a TRAP.

RT-PCR. Total RNA were used as a template for reverse transcription, using the following protocol. Each 20-μl reaction contained 1× Omniscript RT buffer (QIAGen), 500 μM

each of dCTP, dATP, dGTP, and dTTP (QIAGen), 1 μM Oligo dT primer (Ambion), 1 μM random decamer primers (Ambion), 1 unit of Omniscript reverse transcriptase (QIAGen), diethyl pyrocarbonate in water (DEPC-H_2O), and 2 μg of total RNA. Mixtures were incubated at 37°C for 60 min for reverse transcription and then at 92°C for 10 min to inactivate the enzyme. Both incubations were carried out in a DNA Engine Peltier Thermal Cycler (MJ Research). Reaction products were kept at 4°C until ready to be used in the subsequent PCR. PCR was performed according to the following protocol; each 50-μl reaction contained 1× PCR buffer (Promega), 50 μM each of dCTP, dATP, dGTP, and dTTP (Promega), 0.5 μl β-actin primer pair (Ambion), 2.5 unit of Taq Polymerase (Promega), 0.5 μM c-*MYC* or *hTERT* primer (see below), 0.1% DEPC-H_2O, and 2 μl of the reverse transcriptase reaction detailed above.

Primer Sequences. The primer sequences used were: c-*MYC* (upstream), 5′-AGAGAAGCTGGCCTCCTACC-3′; c-*MYC* (downstream), 5′-AGCTTTTGCTCCTCTGCTTG-3′ (product length, 2166 bp); *hTERT* (upstream), 5′-GCCTCT-TCGACGTCTTCCTA-3′; *hTERT* (downstream), 5′-CCCCAA-TTTGACCCACAG-3′ (product length 1493 bp). The reactions were incubated in a DNA Engine Peltier Thermal Cycler as follows: 95°C, 5 min; (95°C, 1 min; 59°C, 1 min, 10 s; 72°C, 1 min, 30 s) 25× for c-*MYC* or 30× for *hTERT*; 72°C, 5 min. PCR products were then kept at 4°C until they were electrophoresed.

Northern Blot Analysis. Selected results obtained by cDNA microarray analysis were confirmed experimentally by Northern Blot analysis. Briefly, equal amounts of total RNA from HeLa S_3 were size separated on a 1% denaturing formaldehyde agarose gel, transferred to a nylon membrane, and hybridized with radiolabeled probes specific to the gene to be analyzed. Probe templates were obtained by PCR amplification of the cDNA insert from the respective IMAGE Consortium clone used on the cDNA microarrays.

Probe Preparation. Human cDNA bacterial clones were purchased from Research Genetics (Huntsville, AL). Referred to as gf200, the set consists of 5184 sequence-validated IMAGE consortium bacterial clones. Approximately 3000 of these clones represent known genes, whereas the remainder are expressed sequence tags. cDNA targets were produced by PCR amplification of the cDNA inserts directly from bacterial cultures. Briefly, individual IMAGE clones were grown in 96-well plates at 37°C for 6 h. One μl of the bacterial culture was added to a 96-well plate containing 45 μl of premixed PCR reaction (Marsh BioProducts, Rochester, NY) and 4 μl of primer (2 μM; Research Genetics). Primers and unincorporated nucleotides were removed after the PCR amplification (initial denaturation step was 96°C for 30 s; followed by 40 cycles of 94°C for 30 s, 55°C for 45 s, and 72°C for 2.5 min) using a 96-well PCR clean-up kit from QIAgen (Valencia, CA). PCR amplification and purification were verified by agarose gel electrophoresis, and PCR product yield was determined using a PicoGreen-based fluorescence assay (Molecular Probes, Eugene, OR) in a 96-well format. Typical yields ranged from 1 to 5 μg. After quantitation, the purified PCR products were dried and resuspended in 10 μl of 2× SSC for printing onto slides.

Microarray Fabrication. cDNAs were printed onto chemically activated glass slides (CEL Industries, Houston, TX) using four quill-type pins (Telechem International, San Jose, CA) mounted onto an OmniGrid robot (GeneMachines, San Carlos, CA). In addition to the 5184 IMAGE clones, a set of 88 human housekeeping genes (Research Genetics), a set of eight *Mesembryanthemum crystallinum* genes, and Cy3 or Cy5 end-labeled oligonucleotides were placed strategically into the array to aid in data normalization, the measurement of nonspecific hybridization, and the identification of the corners of the array, respectively. Additionally, a set of 103 IMAGE clones representing known genes of interest not found in gf200 were purchased from Research Genetics and included in the microarray. After printing, the slides were placed in a humidity chamber overnight in the dark to rehydrate the arrays. The following day, slides were washed for 1 min in 0.1% SDS and 1 min in double-distilled water at room temperature. Slides were then submerged in 240 ml of 75% v/v water/ethanol solution into which 0.6 g of sodium cyanoborohydride had been freshly dissolved. After 5 min at room temperature, slides were washed four times in double-distilled water for 2 min and spun dry at 500 × *g* for 1 min. Slides were stored in the dark at room temperature and <40% humidity until use.

Target Preparation. Fluorescent first-strand cDNA was made from 4 μg of $polyA^+$ RNA in the presence of 50 μM Cy5-dCTP or Cy3-dCTP in a 25-μl volume containing 500 ng of oligo (12–18 dT), 1× Superscript buffer, 400 units of Superscript II, 3.3 units of RNase inhibitor (all from Life Technologies, Inc., Grand Island, NY), 400 μM each of dGTP, dATP, and dTTP, 100 μM dCTP, and 10 mM DTT. All reagents except the Superscript II were mixed on ice and placed at 65°C for 5 min and then at 25°C for 5 min, at which point the Superscript was added, and the mixture was heated to 42°C for 2 h. The mRNA template was hydrolyzed by heating the reaction for 5 min at 95°C, adding 6.25 μl of 1 M NaOH, and incubating for 10 min at 37°C. Neutralization was achieved by the addition of 6.25 μl of 1 M HCl. Labeled cDNA from two reactions (one Cy3 labeled, one Cy5 labeled) was combined and purified on a Microcon-50 column using four buffer exchanges (the first three were double-distilled water, the final exchange was 10 mM Tris-HCl, pH 7.5). After elution from the column, the probe was lyophilized to dryness and resuspended in 10 μl of hybridization buffer (2× SSC, 0.1% SDS, 100 ng/μl *Cot*I DNA, and 100 ng/μl oligo dA), denatured by boiling for 2.5 min, and added to a denatured microarray (slide was boiled for 2 min in double-distilled water, plunged into room temperature ethanol, and spun dry at 500 × *g*). A coverslip (22 × 22 mm) was applied, and the array was placed in a hybridization chamber (GeneMachines) at 62°C for 18 h. After hybridization, slides were washed by placing them into 50-ml conical tubes containing 2× SSC, 0.1% SDS for 5 min; 0.06× SSC, 0.1% SDS for 5 min; and 0.06× SSC for 2 min, all at room temperature. Slides were scanned for Cy3 and Cy5 fluorescence using an Axon GenePix 4000 microarray reader (Axon Instruments, Foster City, CA) and quantitated using GenePix software. The 8226/S and 8226/Dox6 hybridizations were performed three times, and the

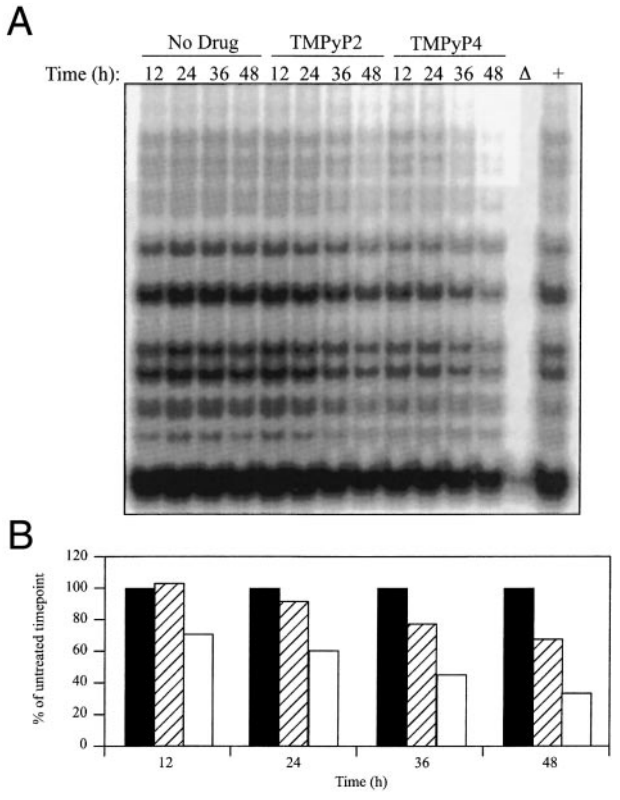

Fig. 2. Telomerase activity after treatment with TMPyP2 and TMPyP4. *A,* MiaPaCa-2 cells were treated in a 75-cm^2 flask at ~50% confluency with water (*No Drug*) 100 μM TMPyP2, or 100 μM TMPyP4 for 12, 24, 36, and 48 h, and the cell lysates were tested for telomerase activity via the TRAPeze assay (Intergen). *B,* telomerase activity was quantified by examining several bands in each lane using ImageQuant software and taking the means of these band densities for each lane. The graph shows the percentage of telomerase activity as compared with the "No Drug" sample (■) for each time point *versus* time of treatment with TMPyP2 (▨) and TMPyP4 (□).

8226/S and 8226/Dox40 hybridizations were performed seven times.

Western Blot Analysis of c-MYC Protein. Depending on protein concentration, 50 μg of protein from each duplicate-treated time point and untreated control were brought up to 40 or 80 μl total volume with NP40 lysis buffer and 10 or 20 μl of 5× SDS-PAGE sample treatment buffer [30% v/v glycerol, 0.3 M Tris (pH 6.8), 10% w/v SDS, 25% v/v 2-mercaptoethanol, and 0.1% w/v bromphenol blue], respectively. These preparations were heated at 100°C for 10 min to denature the proteins and then placed on ice to condense until ready for loading onto the gel. Solutions for 10% Laemmli SDS-polyacrylamide gels were prepared, and gels were poured according to published procedure (33). Depending on the amount of protein loaded, 0.75- or 1.5-mm-thick × 15-cm-long gels were poured, with a 3-cm stacking gel and a 12-cm running gel. Denatured protein solutions were loaded onto the gel, along with 15 μl of Kaleidoscope Protein Standards (Bio-Rad) and resuspended in NP40 lysis buffer to equal the volume of protein loaded. Empty wells were loaded with an equal volume of 5× SDS-PAGE sample treatment buffer diluted in NP40 lysis buffer. Gels were run on an adjustable vertical slab gel apparatus (CBS Scientific Co.) at 100–120 V until the dye front ran off the bottom of the gel. After electrophoresis, gels were cropped of their stacking component and immersed in cold (4°C) Towbin transfer buffer (33). Protran nitrocellulose membrane material (Schleicher and Schuell, Inc.) and 3M Whatman filter paper (Bio-Rad) were cut to match the size of the gels and immersed in cold transfer buffer as well. The transfer stack was assembled according to published procedure (33), and proteins were transferred for 2.5 h in a model EBU-102 transfer tank (CBS Scientific Co.) at 300 mA using an EC-3000P power source (EC Apparatus Corp.). Membranes were blocked overnight with 5% nonfat dry milk in TBS-T and blotted with a 1:1000 dilution of c-MYC monoclonal antibody (Neomarkers) in blocking buffer for 1 h. Membranes were then washed three times in blocking buffer, and bound antibodies were localized with a 1:5000 solution of horseradish peroxidase-labeled goat-antimouse immunoglobulin. Protein bands were then detected using the Phototype-HRP Detection kit (Cell Signaling).

***In Vivo* Activity of TMPyP2 and TMPyP4.** Female nude mice weighing ~20 g were implanted s.c. by trocar injection with MX-1 mammary tumor cells or PC-3 human prostate carcinomas harvested from cell cultures, both of which have elevated c-MYC levels. For each group, 10 mice with tumors were used, each of which was ear tagged and followed individually throughout the experiment. Mice were weighed twice weekly, and tumor measurements were taken by calipers twice weekly, starting on day 1. These tumor measurements were converted to mg tumor weight by $L^2 \times W/2$ (where L is length and W is width), and from these calculated tumor weights the termination date was determined.

In the MX-1 model, after tumors reached a weight of 100 mg, animals were administered cyclophosphamide (150 mg/kg, i.p., q.d. × 1), which left the mice with a minimum of tumor burden. Animals were then pair-matched into groups of eight mice each. Treatment with TMPyP4 (10 and 20 mg/kg, i.p., two times weekly) was then started and continued until the end of the study. Survival, or time to reaching a 2-g tumor size, was the primary efficacy end point of this study.

Animals with PC-3 injected cells were allowed to form tumors of ~60 mg in weight, at which time the animals were pair-matched into treatment and control groups. The administration of drugs or vehicle began the day the animals were pair-matched (day 1), and all injections were done i.p. Porphyrins were formulated for injection in distilled water and administered at 40 mg/kg on a q.d. × 5 schedule. The experiment was terminated when control tumors reached a size of 2 g.

Results

TMPyP4 Reduces Telomerase Activity in Cell Culture. It has already been established that TMPyP4 can bind to and stabilize DNA-G-quadruplex structures in human telomeric sequences (34). Knowing this, we were interested in the effect that this interaction might have on telomerase activity. MiaPaCa-2 cells were treated with 100 μM TMPyP4 for 12,

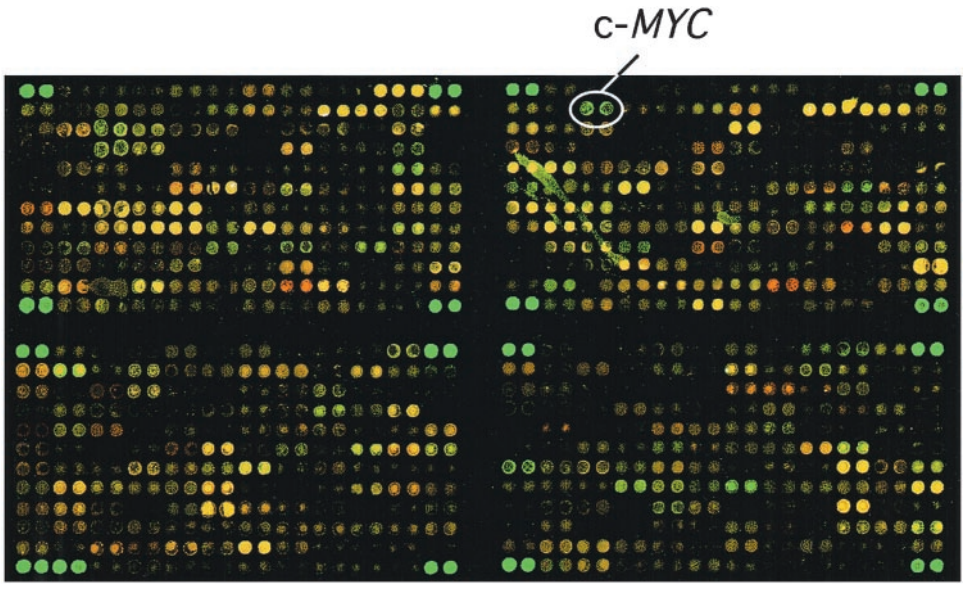

Fig. 3. cDNA microarray analysis of HeLa S_3 cells treated with TMPyP2 or TMPyP4. Cells were treated with 100 μM TMPyP2 or TMPyP4 for 12, 24, 36, and 48 h, and mRNA was extracted and labeled for microarray analysis. A sample slide (TMPyP4-treated, 48 h) is shown, and the c-*MYC* proto-oncogene, the most consistently down-regulated gene in this study, is highlighted. A number of other genes, including c-*MYC*-regulated genes, proto-oncogenes, and cell cycle controllers, were also specifically affected by TMPyP4 (see Tables 1 and 2).

24, 36, and 48 h, and total protein was extracted for use in a TRAP assay. It was found that TMPyP4 could indeed inhibit telomerase activity in a time-dependent manner (Fig. 2). A similar pattern was seen when HeLa cells were treated with TMPyP4 (data not shown). TMPyP2, an analogue of TMPyP4 that is less able to interact with G-quadruplex structures, had a much less pronounced effect on telomerase. This result was unexpected. Because TMPyP4 interacts with G-quadruplexes, it is not obvious why the protein extract from cells treated with the chemical should yield a lower telomerase activity in a TRAP assay. However, this observation was particularly intriguing because TMPyP2, which only poorly interacts with G-quadruplex structures, showed a corresponding lesser effect.

A Comparison of TMPyP2 and TMPyP4 in the cDNA Microarray Shows Specific Down-Regulation of c-*MYC* and Downstream-regulated Genes by TMPyP4. HeLa cells were treated with TMPyP2 or TMPyP4 at 100 μM for 12, 24, 36, and 48 h before isolation of the RNA for microarray analysis. Fig. 3 shows a sample microarray slide for TMPyP4. The results from the TMPyP4 and TMPyP2 microarrays were compared in two ways, as shown in Tables 1 and 2. Table 1 shows those genes whose expression was altered by at least 3-fold by either TMPyP2 or TMPyP4, and Table 2 shows those genes altered only in TMPyP4-treated cells. The results show that a subset of genes is responsive to both TMPyP2 and TMPyP4 treatment (Table 1). These include genes involved in the oxidative stress response (superoxide dismutase) and metallothionein genes. A number of genes were also affected uniquely by TMPyP4. This group includes the proto-oncogene c-*MYC* as well as several c-*MYC*-regulated genes. Other cell cycle regulators and proto-oncogenes were also influenced by TMPyP4 treatment (Table 2). It is of interest that among these uniquely affected genes are the proto-oncogenes c-*FOS* and c-*MYB*, which have been shown, along with c-*MYC*, to contain sequences in their promoters conducive to the formation of G-quadruplex structures (6).

TMPyP4 Causes a Decrease in c-*MYC* Expression. To verify the effect on c-*MYC* expression by TMPyP4, Northern Blot analysis was performed for the c-*MYC* transcript. HeLa S_3 cells were treated with 100 μM TMPyP4 for 12, 24, 36, and 50 h, and the total RNA was extracted, electrophoresed, and used as a target for Northern Blot analysis, with labeled c-*MYC* cDNA as a probe. The results are shown in Fig. 4. As is evident, there is an overall decrease in the abundance of c-*MYC* mRNA with continued exposure to TMPyP4.

TMPyP4 Causes a Decrease in the Expression of c-*MYC* and *hTERT*. Having shown an inhibitory effect of TMPyP4 on c-*MYC* expression in HeLa cells, we wanted to determine whether this effect would be carried over to other cell lines. Moreover, because hTERT, the catalytic subunit of telomerase, is partially under the control of c-*MYC*, we were curious as to the effect of TMPyP4 on the expression of this gene as well. MiaPaCa-2 pancreatic cancer cells were treated with 100 μM TMPyP2 or TMPyP4 for 12, 24, 36, and 48 h, and the total RNA was extracted and subjected to poly(A)-specific reverse transcription to generate cDNA. This cDNA was then used as a template for specific PCR amplification of the c-*MYC* and *hTERT* sequences, as described in "Materials and Methods." The results are shown in Fig. 5. The inhibitory effect of TMPyP4 on the expression of both of these genes is quite obvious; there is significant effect at 12 h on both *hTERT* and c-*MYC*, which is maintained over a 48-hour period as assayed by RT-PCR. TMPyP2, on the other hand, has a much less pronounced effect on these two genes. A similar pattern of gene down-regulation for both c-*MYC* and *hTERT* was seen in HeLa cells when these cell lines were treated with these two porphyrins.[5] Because *hTERT* is under transcriptional control in part by the c-MYC transcription factor (13–15), parallel effects on c-*MYC* and

[5] C. L. Grand, H. Han, R. M. Muñoz, D. D. Von Hoff, L. H. Hurley, and D. J. Bearss, unpublished results.

Table 1 Genes affected by both TMPyP4 and TMPyP2 treatment

Induced genes	Down-regulated genes
Oxidation reduction genes	Metallothionein genes
Cystathionase	*Metallothionein 2H*
Lactate dehydrogenase	*Metallothionein 1L*
Cytochrome p450	*Metallothionein IH*
Thioredoxin	*Metallothionein 2A*
Superoxide dismutase-1	
Superoxide dismutase-2	
Glutathione S-transferase M4	
Proteasome genes	
Macropain	
Macropain 26S	

Table 2 Effects of TMPyP4 treatment on gene expression

Induced genes	Down-regulated genes
Apoptosis genes	c-*MYC*-associated genes
Caspase 1	c-*MYC*
	Ornithine decarboxylase
	CDC25A
Cell signaling genes	Cell cycle genes
TGF-β	*CDK-4*
CD47	*CDK-6*
CD9	*Cyclin B1*
CO-29	
RAB-1A	
RAB9	
Proliferation-associated gene A	
DNA repair genes	Cell signaling and oncogenes
MLH1	c-*FOS*
ERCC5	c-*MYC*
	JUN-B
	c-*MYB*
	STAT-1
Heat shock genes	Oxidation reduction genes
HSP27	*Cytochrome C1*
HSP10	

hTERT are expected. Furthermore, this likely explains the apparent inhibition of telomerase we observed in earlier experiments using the TRAP assay.

TMPyP4 Causes a Decrease in c-MYC Protein Expression. A Western Blot analysis was performed to determine whether there was a corresponding decrease in the c-MYC protein levels. MiaPaCa-2 pancreatic cancer cells were treated with 100 μM TMPyP2 or TMPyP4 for 12, 24, 36, and 48 h, the total protein was extracted and electrophoresed by SDS-PAGE, and the electrophoresed protein was used as a target for Western Blot analysis. A monoclonal antibody to human c-MYC was used as a probe to specifically detect this transcription factor. The results are shown in Fig. 6*A*. Parallel with the RT-PCR and Northern Blot analysis results presented earlier, TMPyP4 caused a decrease in the amount of c-MYC protein present. TMPyP2 had an insignificant effect.

TMPyP4 Is Able to Slow the Growth of Human Breast (MX-1) and Prostate Tumor (PC-3) Xenografts in Mice. The models chosen for evaluation of TMPyP4 were the MX-1 mammary chemoadjuvant model and a PC-3 prostate model, both of which have elevated c-*MYC* levels and high telomerase activity (35). In the MX-1 model, after tumors reached 100 mg, animals were administered cyclophosphamide (150 mg/kg, i.p., q.d. $\times$ 1), which left the mice with a minimum of tumor burden. Animals were then pair-matched into groups of 20 mice each. Treatment (day 1) with TMPyP4 (10 and 20 mg/kg, i.p., two times weekly) was then started and continued until the end of study. Survival, or time to reaching a 2-g tumor size, was the primary efficacy end point of this study. This study design was developed to simulate a clinically relevant condition that occurs in women with breast cancer after aggressive cytotoxic therapy.

The data in Fig. 7*A* show the survival curve for animals administered vehicle *versus* TMPyP4 at 10 mg/kg (i.p., two times weekly). Treatment with TMPyP4 resulted in an increase in survival compared with controls. At days 60 and 100, survival was 70% *versus* 45% and 55% *versus* 45% for animals administered TMPyP4 *versus* vehicle, respectively. Treatment with TMPyP4 at 20 mg/kg (i.p., two times weekly) was stopped at day 60 because of toxicity (data set not shown).

We have also evaluated TMPyP2 *versus* TMPyP4 in a PC-3 prostate carcinoma model in which c-*MYC* is overexpressed. In this model, animals were not pretreated with a cytotoxic agent. Tumor weights were evaluated at days 1, 4, 8, 11, 15, and 18, and mean tumor growth rates were calculated (Fig. 7*B*). Control tumors grew at a rate of 132 $\pm$ 15 mg/day, whereas TMPyP2 and TMPyP4 treatment slowed tumor growth to 104 $\pm$ 16 mg/day and 50 $\pm$ 6 mg/day, respectively. Only TMPyP4 caused a significant decrease in mean tumor growth rates ($P < 0.05$ by ANOVA).

In summary, we have clearly documented that TMPyP4 has activity in an adjuvant model of breast cancer and standalone activity in PC-3. Significantly, c-*MYC* is overexpressed in both MX-1 and PC-3.

Discussion

Previous studies from our group have shown that the cationic porphyrin TMPyP4 can bind to and stabilize G-quadruplexes formed in human telomeric sequences, thus interfering with the ability of telomerase to extend telomeric DNA repeats (8). We have also shown, in this and previous studies, that TMPyP4 reduces telomerase activity in cell extracts. This is in contrast to TMPyP2, which has a much less pronounced effect on the activity of telomerase. This suggests that the effects of TMPyP4 may not be limited to its interaction with telomeric G-quadruplexes.

To better understand the mechanistic basis of the observed effects of TMPyP2 and TMPyP4 on telomerase activity, we have examined changes in gene expression after treatment with these compounds. The expression levels of a number of genes, as determined by cDNA microarray analysis, were found to be changed by treatment with these molecules. A subset of genes was affected by both porphyrins. These genes are related to oxidative stress response, indicating that treatment with these porphyrins may result in oxidative damage. This is not surprising, because porphyrins in general have been used in photodynamic therapy for their ability to produce reactive oxygen (36); however, attempts were made to minimize the exposure of treated cells to light. Another group of genes was altered uniquely by TMPyP4,

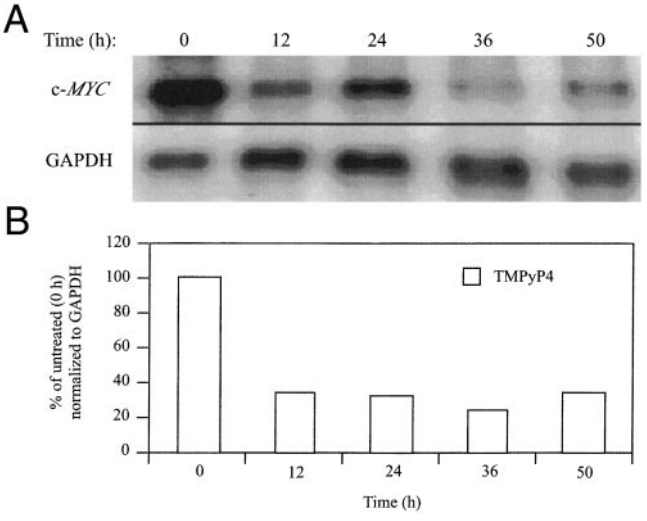

Fig. 4. Northern Blot analysis of c-*MYC* mRNA after treatment with TMPyP4. *A,* HeLa S_3 cells were treated with 100 μM TMPyP4 for 0, 12, 24, 36, and 50 h, and the cellular RNA was probed by Northern Blot with either labeled c-*MYC* mRNA or labeled GAPDH mRNA (control). *B,* band intensity was quantified using ImageQuant software, and c-*MYC* band intensities were normalized to GAPDH intensity. The graph shows the percentage of c-*MYC* expression, normalized to GAPDH, as compared with the untreated (0 h) time point *versus* time of treatment with TMPyP4.

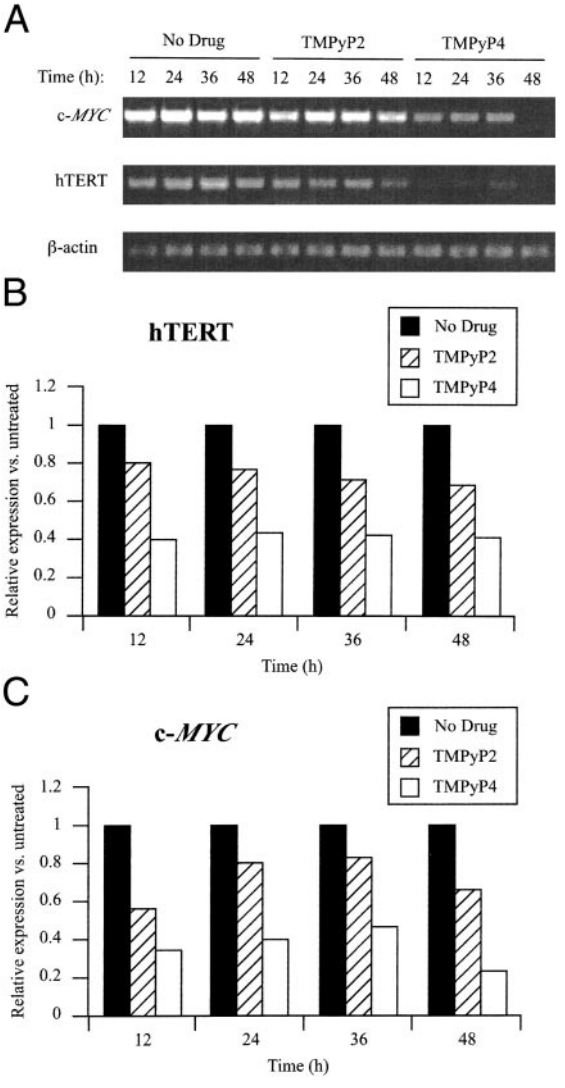

Fig. 5. RT-PCR to determine the effect of TMPyP2 and TMPyP4 on c-*MYC* and *hTERT* mRNA levels. *A,* MiaPaCa-2 cells were treated in a 75-cm^2 flask at ~50% confluency with water (*No Drug*), 100 μM TMPyP2, or 100 μM TMPyP4 for 12, 24, 36, and 48 h, and the total RNA was extracted and subjected to reverse transcription followed by PCR for c-*MYC*, *hTERT*, or β-actin (control). *B, hTERT* expression was quantified using ImageQuant software and normalized to β-actin expression. The graph shows relative expression of *hTERT* as compared with the "No Drug" sample for each time point *versus* time of treatment with TMPyP2 and TMPyP4. *C,* c-*MYC* expression was quantified using ImageQuant software and normalized to β-actin expression. The graph shows relative expression of c-*MYC* as compared with the "No Drug" sample for each time point *versus* time of treatment with TMPyP2 and TMPyP4.

including a number of cell cycle regulatory genes and proto-oncogenes. Most interestingly, these data show that TMPyP4 can reduce the expression of the c-*MYC* oncogene as well as several c-*MYC*-regulated genes, implicating c-*MYC* down-regulation as a potential target pathway for TMPyP4. This is of particular interest in light of the fact that the catalytic subunit of telomerase, hTERT, is transcriptionally regulated by c-MYC. Therefore, because TMPyP4 inhibits c-*MYC* expression and hTERT is controlled by this transcription factor, this explains the effect of TMPyP4 on telomerase activity.

We confirmed this model by showing that TMPyP4 decreases c-*MYC* expression at the RNA and protein levels in MiaPaCa-2 and HeLa S_3 cells. In contrast, TMPyP2 had a much reduced effect in all of these assays compared with TMPyP4. TMPyP2 has a much lesser ability to bind to and stabilize G-quadruplex DNA structures (34), suggesting to us that the unique effects of TMPyP4 on gene expression may be mediated through an interaction with such a secondary DNA structure. The c-*MYC* promoter region contains a stretch of guanine-rich DNA (the NHE III_1) that can form G-quadruplexes. Human telomeres, with their repeats of the hexanucleotide $(TTAGGG)_n$, also have the potential to form G-quadruplexes. Of considerable interest to us now is the mechanism by which TMPyP4 mediates its effects on c-*MYC* and telomerase and whether this is related to the binding of TMPyP4 to G-quadruplex structures in the NHE III_1.

The inhibition of c-*MYC* expression *in vitro* by TMPyP4 accounts for at least part of the reduction of telomerase activity by this molecule. The c-*MYC* proto-oncogene, as mentioned earlier, plays a role in the expression of hTERT, the catalytic subunit of the telomerase holoenzyme (13–15). This is likely not the only mechanism of telomerase inhibition by TMPyP4, however. It has been demonstrated previously that TMPyP4 can inhibit telomerase activity in a cell-free system using the direct assay (IC_{50}, 6 μM; Ref. 37). This suggests that TMPyP4 could be interacting with either the telomere or the telomerase holoenzyme complex itself.

In support of the observations made here of down-regulation of c-*MYC* and *hTERT*, it has also been demonstrated that in multiple myeloma cells there is more pronounced telomere shortening and apoptosis by TMPyP4 than by TMPyP2.[3]

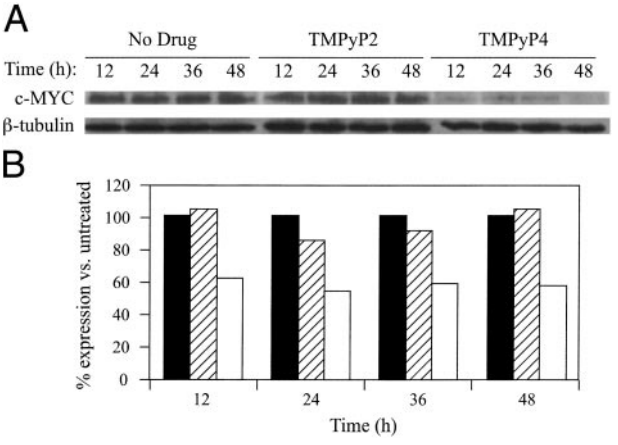

Fig. 6. Western Blot analysis of c-MYC protein after treatment with TMPyP2 and TMPyP4. *A,* MiaPaCa-2 cells were treated in a 75-cm^2 flask at ~50% confluency with water (*No Drug*), 100 μM TMPyP2, or 100 μM TMPyP4 for 12, 24, 36, and 48 h, and the total protein was extracted and probed by Western Blot with mouse anti-c-MYC or mouse anti-β-actin antibody. *B,* c-MYC protein was quantified using ImageQuant software and normalized to β-actin protein. The graph shows the percentage of c-MYC protein as compared with the "No Drug" sample (■) for each time point *versus* time of treatment with TMPyP2 (▨) and TMPyP4 (□).

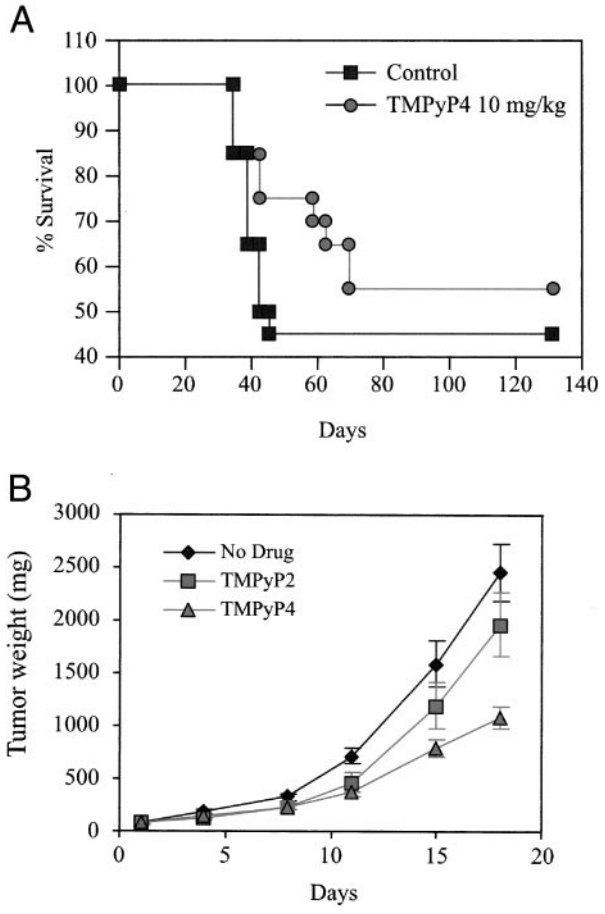

Fig. 7. *A,* percent survival of TMPyP4 *versus* MX-1 adjuvant human breast tumor xenograft. Tumors were allowed to reach 100 mg, and mice were treated with 150 mg/kg cyclophosphamide, pair-matched into groups of 20 mice each, and treated with or without 10 mg/kg TMPyP4. At day 60, survival was improved from 45 to 75% with TMPyP4 treatment and from 45 to 55% at day 100. *B,* slowing of tumor growth in PC-3 by TMPyP4. Tumors were allowed to reach a weight of 100 mg before treatment with or without 10 mg/kg TMPyP2 or TMPyP4, and tumor weight measurements were taken at days 1, 4, 8, 11, 15, and 18. Mean tumor growth rates were calculated to be 132 $\pm$ 15 mg/day for control mice, 104 $\pm$ 16 mg/day for TMPyP2-treated mice, and 50 $\pm$ 6 mg/day for mice treated with TMPyP4. A significant inhibition ($P < 0.05$) was seen only with TMPyP4 treatment.

As further validation of the potential anticancer activity of G-quadruplex-interactive agents, we performed *in vivo* studies in mice, using two well-established tumor models. TMPyP4 was tested as a stand-alone agent and in an adjuvant chemotherapy model with a cytotoxic compound, cyclophosphamide, and we found in both cases that TMPyP4 was able to prolong survival and decrease tumor growth, compared with TMPyP2 and untreated controls. These results are significant, given that TMPyP4 has low cytotoxicity *in vitro* (8), suggesting that TMPyP4 acts as a cytostatic agent. These results also suggest that the effects of TMPyP4 are mediated through a G-quadruplex-dependent mechanism, because treatment with TMPyP2 showed no significant effects on reduction of tumor growth. Blackburn *et al.* (38) has proposed a telomere capping function for telomerase and that simultaneous telomere injury and depletion of telomerase may have more detrimental effects than either event alone. Agents such as TMPyP4 that fortunately have both effects (*i.e.,* telomere injury through G-quadruplex formation and down-regulation of hTERT) may be more efficacious than other agents that only affect telomeres.

Both the c-MYC and telomerase proteins are valuable targets for anticancer drug development, because both are abnormally overexpressed in a very substantial proportion of human malignancies. We have found that the cationic porphyrin TMPyP4 is not only able to down-regulate the expression and activity of both of these gene products but also has significant antitumor activity *in vivo*, making it a worthwhile lead compound for further development.

Acknowledgments

We are grateful to Dr. David M. Bishop for proofreading and editing the manuscript and for preparing the final version of the figures.

References

1. Hurley, L. H., Wheelhouse, R. T., Sun, D., Kerwin, S. M., Salazar, M., Fedoroff, O. Yu., Han, F. X., Han, H., Izbicka, E., and Von Hoff, D. D. G-quadruplexes as targets for drug design. Pharmacol. Ther., *85:* 141–158, 2000.

2. Henderson, E., Hardin, C. C., Walk, S. K., Tinoco, I., Jr., and Blackburn, E. H. Telomeric DNA oligonucleotides form novel intramolecular structures containing guanine-guanine base pairs. Cell, *51:* 899–908, 1987.

3. Sundquist, W. I., and Klug, A. Telomeric DNA dimerizes by formation of guanine tetrads between hairpin loops. Nature (Lond.), *342:* 825–829, 1989.

4. Blackburn, E. Structure and function of telomeres. Nature (Lond.), *350:* 569–573, 1991.

5. Zahler, A. M., Williamson, J. R., Cech, T. R., and Prescott, D. M. Inhibition of telomerase by G-quartet DNA structures. Nature (Lond.), *350:* 718–720, 1991.

6. Simonsson, T. DNA tetraplex formation in the control region of c-myc. Nucleic Acids Res., *26:* 1167–1172, 1998.

7. Simonsson, T., and Sjoback, R. DNA tetraplex formation studied with fluorescence resonance energy transfer. J. Biol. Chem., *274:* 17379–17383, 1999.

8. Izbicka, E., Wheelhouse, R. T., Raymond, E., Davidson, K. K., Lawrence, R. A., Sun, D., Windle, B. E., Hurley, L. H., and Von Hoff, D. D. Effects of cationic porphyrins as G-quadruplex interactive agents in human tumor cells. Cancer Res., *59:* 639–644, 1999.

9. Izbicka, E., Nishioka, D., Marcell, V., Raymond, E., Davidson, K. K., Lawrence, R. A., Wheelhouse, R. T., Hurley, L. H., Wu, R. S., and Von Hoff, D. D. Telomere-interactive agents affect proliferation rates and induce chromosomal destabilization in sea urchin embryos. Anti-Cancer Drug Des., *14:* 355–365, 1999.

10. Fedoroff, O. Yu., Rangan, A., Chemeris, V. V., and Hurley, L. H. Cationic porphyrins promote the formation of i-motif DNA and bind peripherally by a nonintercalative mechanism. Biochemistry, *39:* 15083–15090, 2000.

11. Ahmed, S., Kintanar, A., and Henderson, E. Human telomeric C-strand tetraplexes. Nat. Struct. Biol., *1:* 83–88, 1994.

12. Gehring, K., Leroy, J. L., and Gueron, M. A tetrameric DNA structure with protonated cytosine·cytosine base pairs. Nature (Lond.), *363:* 561–565, 1993.

13. Hahn, W. C., and Meyerson, M. Telomerase activation, cellular immortalization and cancer. Ann. Med., *33:* 123–129, 2001.

14. Wang, J., Xie, L. Y., Allan, S., Beach, D., and Hannon, G. J. Myc activates telomerase. Genes Dev., *12:* 1769–1774, 1998.

15. Wu, K. J., Grandori, C., Amacker, M., Simon-Vermot, N., Polack, A., Lingner, J., and Dalla-Favera, R. Direct activation of TERT transcription by c-MYC. Nat. Genet., *21:* 220–224, 1999.

16. Dang, C. V. c-Myc target genes involved in cell growth, apoptosis, and metabolism. Mol. Cell. Biol., *19:* 1–11, 1999.

17. Dang, C. V., Resar, L. M., Emison, E., Kim, S., Li, Q., Prescott, J. E., Wonsey, D., and Zeller, K. Function of the c-Myc oncogenic transcription factor. Exp. Cell Res., *253:* 63–77, 1999.

18. Grandori, C., and Eisenman, R. N. Myc target genes. Trends Biochem. Sci., *22:* 177–181, 1997.

19. Henriksson, M., and Luscher, B. Proteins of the Myc network: essential regulators of cell growth and differentiation. Adv. Cancer Res., *68:* 109–182, 1996.

20. Marcu, K. B., Bossone, S. A., and Patel, A. J. Myc function and regulation. Annu. Rev. Biochem., *61:* 809–860, 1992.

21. Fahrlander, P. D., Sumegi, J., Yang, J. Q., Wiener, F., Marcu, K. B., and Klein, G. Activation of the c-*myc* oncogene by the immunoglobulin heavy-chain gene enhancer after multiple switch region-mediated chromosome rearrangements in a murine plasmacytoma. Proc. Natl. Acad. Sci. USA, *82:* 3746–3750, 1985.

22. Mullins, J. I., Brody, D. S., Binari, R. C., Jr., and Cotter, S. M. Viral transduction of c-*myc* gene in naturally occurring feline leukaemias. Nature (Lond.), *308:* 856–858, 1984.

23. Fulton, R., Forrest, D., McFarlane, R., Onions, D., and Neil, J. C. Retroviral transduction of T-cell antigen receptor β-chain and *myc* genes. Nature (Lond.), *326:* 190–194, 1987.

24. Neil, J. C., Hughes, D., McFarlane, R., Wilkie, N. M., Onions, D. E., Lees, G., and Jarrett, O. Transduction and rearrangement of the *myc* gene by feline leukaemia virus in naturally occurring T-cell leukaemias. Nature (Lond.), *308:* 814–820, 1984.

25. Alitalo, K., Schwab, M., Lin, C. C., Varmus, H. E., and Bishop, J. M. Homogeneously staining chromosomal regions contain amplified copies of an abundantly expressed cellular oncogene (c-*myc*) in malignant neuroendocrine cells from a human colon carcinoma. Proc. Natl. Acad. Sci. USA, *80:* 1707–1711, 1983.

26. Graham, M., Adams, J. M., and Cory, S. Murine T lymphomas with retroviral inserts in the chromosomal 15 locus for plasmacytoma variant translocations. Nature (Lond.), *314:* 740–743, 1985.

27. Cole, M. D. The *myc* oncogene: its role in transformation and differentiation. Annu. Rev. Genet., *20:* 361–384, 1986.

28. Henriksson, M., Selivanova, G., Lindstrom, M., and Wiman, K. G. Inactivation of Myc-induced p53-dependent apoptosis in human tumors. Apoptosis, *6:* 133–137, 2001.

29. Boxer, L. M., and Dang, C. V. Translocations involving c-myc and c-myc function. Oncogene, *20:* 5595–5610, 2001.

30. Siebenlist, U., Hennighausen, L., Battey, J., and Leder, P. Chromatin structure and protein binding in the putative regulatory region of the c-*myc* gene in Burkitt lymphoma. Cell, *37:* 381–391, 1984.

31. Berberich, S. J., and Postel, E. H. PuF/NM23–H2/NDPK-B transactivates a human c-myc promoter-*CAT* gene via a functional nuclease hypersensitive element. Oncogene, *10:* 2343–2347, 1995.

32. Simonsson, T., Pribylova, M., and Vorlickova, M. A nuclease hypersensitive element in the human c-myc promoter adopts several distinct i-tetraplex structures. Biochem. Biophys. Res. Commun., *278:* 158–166, 2000.

33. Instruments, H. S. Protein Electrophoresis Applications Guide, p. 106. San Francisco: Hoefer Scientific Instruments, 1994.

34. Han, F. X., Wheelhouse, R. T., and Hurley, L. H. Interactions of TMPyP4 and TMPyP2 with quadruplex DNA. Structural basis for the differential effects on telomerase inhibition. J. Am. Chem. Soc., *121:* 3561–3570, 1999.

35. Raymond, E., Sun, D., Chen, S. F., Windle, B., and Von Hoff, D. D. Agents that target telomerase and telomeres. Curr. Opin. Biotechnol., *7:* 583–591, 1996.

36. Granville, D. J., McManus, B. M., and Hunt, D. W. Photodynamic therapy: shedding light on the biochemical pathways regulating porphyrin-mediated cell death. Histol. Histopathol., *16:* 309–317, 2001.

37. Sun, D., Thompson, B., Cathers, B. E., Salazar, M., Kerwin, S. M., Trent, J. O., Jenkins, T. C., Neidle, S., and Hurley, L. H. Inhibition of human telomerase by a G-quadruplex-interactive compound. J. Med. Chem., *40:* 2113–2116, 1997.

38. Blackburn, E. H. Switching and signaling at the telomere. Cell, *106:* 661–673, 2001.